

ON SOME PROBLEMS IN DETERMINING TENSILE PARAMETERS OF CONCRETE MODEL FROM SIZE EFFECT TESTS

Ireneusz Marzec

Jerzy Bobiński

Gdansk University of Technology, Poland

ABSTRACT

The paper presents results of numerical simulations of size effect phenomenon in concrete specimens. The behaviour of in-plane geometrically similar notched and unnotched beams under three-point bending is investigated. In total 18 beams are analysed. Concrete beams of four different sizes and five different notch to depth ratios are simulated. Two methods are applied to describe cracks. First, an elasto-plastic constitutive law with a Rankine criterion and an associated flow rule is defined. In order to obtain mesh independent results, an integral non-local theory is used as a regularisation method in the softening regime. Alternatively, cracks are described in a discrete way within Extended Finite Element Method (XFEM). Two softening relationships in the softening regime are studied: a bilinear and an exponential curve. Obtained numerical results are compared with experimental outcomes recently reported in literature. Calculated maximum forces (nominal strengths) are quantitatively verified against experimental values, but the force – displacement curves are also examined. It is shown that both approaches give results consistent with experiments. Moreover, both softening curves with different initial fracture energies can produce similar force-displacement curves.

Keywords: Concrete, Size effect, Fracture energy, elasto-plasticity, XFEM

INTRODUCTION

Concrete is one of the most popular materials used in civil engineering to erect buildings, bridges and other structures on land and various port facilities like breakwaters or quays. Its tensile strength is several times smaller than compressive one, therefore it is usually applied with steel reinforcing bars. These bars are responsible to carry (mostly) tensile stresses, while the concrete itself sustains compressive stresses, and the tensile strength of concrete is neglected. The situation is different in plain or weakly reinforced massive concrete structures in civil or coastal engineering, like foundations, dams etc. The tensile strength of concrete cannot be neglected

and the proper estimation of the concrete's properties in tension is of great importance.

One of the salient phenomenon observed in concrete structures is the presence of size effect. The strength (and other properties) of material depends on the size of a specimen examined; small elements have a greater nominal strength than bigger ones. It is caused by the existence of the so-called fracture process zone (FPZ), which size is not negligible comparing to the size of the specimen. Deformations localise inside these zones; at the beginning as a set of diffused micro-cracks and later a discrete macro-crack. The observed size effect results are placed between plastic limit theory and linear elastic fracture mechanics solutions. Therefore, the proper theoretical capture of the size effect phenomenon is crucial

when experimental results from tests performed on small specimens are to be extrapolated into bigger ones.

Within continuum mechanics, cracks can be described as a smeared (continuous), discrete (discontinuous) or by coupling these two approaches (Mazars et al. [20], Marzec et al. [18], Unger et al. [26], Bobiński and Tejchman [5]). The first (smeared) approach defines a crack as region (band) with a certain width, while in the second formulation it is presented as a line (surface) with zero thickness and assumed displacement jump across. When using classical constitutive laws with strain softening, a mesh dependency is observed. In order to obtain mesh independent results and to restore the well-posedness of the boundary value problem, a regularisation method is needed. This enrichment introduces a characteristic length of the microstructure into the macroscopic material description. It can be done via a non-local theory, gradient terms or using viscosity in dynamic problems (Brinkgreve [6], Glema et al. [10], Marzec et al. [19], Wang et al. [27], Winnicki et al. [29]). More sophisticated formulations couple continuous and discontinuous descriptions (Simone et al. [22, 23]). Non-locality can be also introduced via fractional differential operators (Beda [3], Błaszczuk [4], Lazopoulos i Lazopoulos [17], Sumelka [24], Sumelka et al. [25]).

Despite a huge amount of performed experiments on concrete specimens, there is still no consensus in describing the fracture process in concrete. Due to several factors influencing the results and a small number of specimens tested in a single experimental programme, it is very hard to properly compare the obtained results and to form general conclusions. Therefore, some experimental campaigns were executed recently to overcome these limitations. Hoover et al. [15] examined in plane geometrically scaled unnotched and notched concrete beams under three-point bending. Four different beam sizes and five different notch to depth ratios were analysed. In total 18 different geometries were defined and more than one hundred specimens were tested. Çağlar and Şener [7] examined geometrically identical beams (80 specimens), but cast in a horizontal position. A slightly smaller number of beams (34 specimens) was tested by Grégoire et al. [12]. They analysed beams of four different sizes and three different notch to depth ratios (unnotched and notched).

Different constitutive laws were used later to reproduce obtained experimental results. Hoover and Bažant [16] used the crack band and a bilinear softening law. They stated that an exponential softening curve was not able to give realistic results. Grégoire et al. [12] applied the isotropic damage constitutive law coupled with the integral non-local theory and an exponential curve defined in softening. A similar model was used in numerical simulations presented by Havlásek et al. [13]. In addition, they studied standard and distance based averaging methods in non-locality.

In the paper, numerical simulations of size effect in plain concrete beams under bending are presented. Two alternative crack descriptions are used: a smeared one via an elasto-plastic with a Rankine criterion enriched by a non-local theory in the softening regime and a discrete one within

XFEM. The influence of defined softening curve and assumed value of the initial fracture energy in both approaches on the obtained results is investigated. Such vast analysis with two different crack descriptions and two different softening curves has not been performed yet. In addition, the deficiencies of the initial fracture energy are pointed out. Numerical results are compared with experimental outcomes.

The paper is organised as follows. The constitutive models are described in Section 2. The problem data are given in Section 3. Obtained results and discussion are presented in Section 4. Conclusions and final remarks are listed in Section 5.

CONSTITUTIVE LAWS

ELASTO-PLASTICITY

As a first option, a smeared description of cracks in concrete is used. An elasto-plastic constitutive law with the classical Rankine criterion is proposed. The yield criterion in 2D is postulated as

$$f = \max\{\sigma_1, \sigma_2\} - \sigma_t(\kappa_C) \quad (1)$$

where:

σ_1, σ_2 – the principal stresses,

σ_t – the tensile yield stress,

κ_C – the softening state variable.

The tensile yield stress σ_t is defined in Sec. 2.3 and the state variable κ_C is equal to the maximum principal plastic strain. Plastic strains are calculated assuming an associated flow rule.

When defining strain softening with the standard constitutive laws, classical finite element calculations fail. Obtained result are mesh dependent and a regularisation method is required to restore the well posedness of the boundary value problem. Here, an integral non-local theory is applied. Non-local rates of state variables $d\kappa_C$ are evaluated as (after Brinkgreve [6])

$$d\bar{\kappa}_C(\mathbf{x}) = (1-m)d\kappa_C(\mathbf{x}) + md\hat{\kappa}_C(\mathbf{x}) \quad (2)$$

where:

\mathbf{x} – point under consideration,

m – non-locality parameter,

$d\hat{\kappa}_C$ – rate of averaged state variable.

The non-locality parameter m should be greater than 1 to effectively apply the non-local theory with elasto-plasticity (so called over-non-local formulation). The rate of averaged state variable is calculated as:

$$d\hat{\kappa}_C(\mathbf{x}) = \frac{\int_V \omega(\|\mathbf{x} - \boldsymbol{\xi}\|) d\kappa_C(\boldsymbol{\xi}) d\boldsymbol{\xi}}{\int_V \omega(\|\mathbf{x} - \boldsymbol{\xi}\|) d\boldsymbol{\xi}} \quad (3)$$

where:

V – volume of the integration domain,

$\boldsymbol{\xi}$ – surrounding point coordinates,

ω – the weighting function.

The weighting function reflects the influence of the surrounding points on the material's behaviour in the considered point \mathbf{x} . Here a Gauss distribution is applied:

$$\omega(r) = \frac{1}{l\sqrt{\pi}} \exp\left(-\left(\frac{r}{l}\right)^2\right) \quad (4)$$

where:

r – the distance between points,

l – the characteristic length.

The characteristic length is the link with the micro-structure of the material. The characteristic length l (but also the non-locality parameter m , the definition of the weight function ω and the formulation of the constitutive law) influences the width of the localisation zone, which in general depends on concrete mesostructure. The averaging in Eqn. (4) is restricted only to a small neighbourhood around a point considered (the influence of points at the distance of $r=3l$ is only of 0.01%). Therefore, although the weight function ω defined in Eqn (4) has unbounded support, only points at the distance no larger than $r=3l$ from the integration domain V . For points \mathbf{x} lying close to the boundary, only points lying within a circle with a radius $r=3l$ and belonging to the specimen are taken into account (see Fig. 1a). In both cases, the denominator in Eqn (3) normalises the averaging operation; the uniform local field remains unchanged after applying the Eqn (3). Near notches so called “shading effect” is taken into account (Fig. 1b).

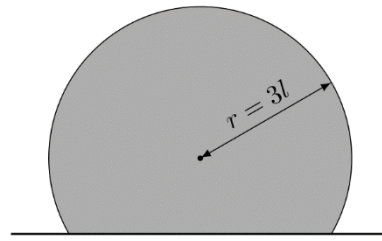
EXTENDED FINITE ELEMENT METHOD

As an alternative approach, cracks can be described as displacement jumps within continuum. In the paper eXtended Finite Element Method (XFEM) is utilised. It is based on a local partition of the unity (PUM) concept by (Melenk and Babuška [21]). It enables adding ‘ad hoc’ extra terms to a standard FE displacement field interpolation to capture displacement jumps across a crack. As a consequence, cracks can be placed through elements; they do not have to follow elements’ edges.

In the paper the formulation (with minor improvements and modifications) proposed by Wells and Sluys [28] for cohesive cracks is adopted. The only major change is the application of the so-called shifted-basis enrichment proposed by Zi and Belytschko [30]. Theoretically, this improvement is equivalent to the classical model, but it simplifies the

implementation (only two types of finite elements exist and total nodal displacements are equal to the standard ones).

a)



b)

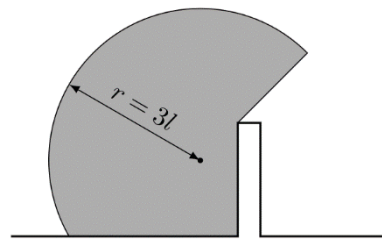


Fig. 1. Averaging domain (grey area) for a point near boundary (a) and close to a notch (b)

Two constitutive relationships have to be declared to describe the behaviour of the material. Outside a crack in a solid (bulk) body a linear elasticity law is assumed. Along the crack a constitutive law between displacement jumps $[[\mathbf{u}]]$ and tractions \mathbf{t} is postulated. The following loading function is assumed:

$$f([[u_n]], \kappa_D) = [[u_n]] - \kappa_D \quad (5)$$

where:

$[[u_n]]$ – normal component of $[[\mathbf{u}]]$,

κ_D – the softening state variable.

The state variable κ_D is calculated as a maximum crack opening $[[u_n]]$ attained during the load history. In active loading (growth of the crack opening) the normal traction t_n is equal to the yield traction t_y defined as:

$$t_y = D_f \sigma_t \quad (6)$$

where:

D_f – correction term,

σ_t – the yield stress defined in Sec. 2.3.

The correction term D_f improves the performance of the model in tension-compression transition cases. It is defined as:

$$D_f = 1 - \exp\left(-\kappa_D \frac{d_f f_t}{G_F}\right) \quad (7)$$

where:

d_f – the drop factor (Cox [8]),

f_t – the tensile strength,

G_F – the total fracture energy.

In unloading/reloading a return to the origin (damage formulation) is assumed:

$$t_n = \frac{t_y}{\kappa_D} [[u_n]] \quad (8)$$

In compression a penalty stiffness is taken. It is calculated as:

$$T_n = \frac{d_f f_t^2}{G_F} \quad (9)$$

In tangential direction, a linear dependence between shear tractions t_s and tangential displacement jump $[[u_s]]$ is assumed:

$$t_s = T_s \frac{t_y}{f_t} [[u_s]] \quad (10)$$

where:

T_s – the initial shear stiffness.

SOFTENING CURVES

In both smeared and discrete crack descriptions two softening curves are used in the numerical simulations. In the present section, symbol κ should be taken either as the state variable κ_C or as the state variable κ_D . First, a bilinear relationship is taken (Fig. 2a):

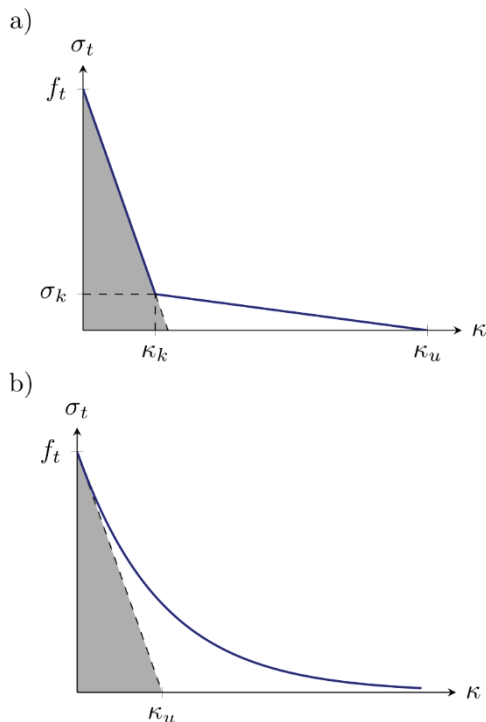


Fig. 2. Bilinear (a) and exponential (b) softening curves (grey area – initial fracture energy)

$$\sigma_y(\kappa) = \begin{cases} f_t + (\sigma_k - f_t) \frac{\kappa}{\kappa_k} & \kappa < \kappa_k \\ \sigma_k \frac{\kappa_u - \kappa}{\kappa_u - \kappa_k} & \kappa_k \leq \kappa < \kappa_u \\ 0 & \kappa \geq \kappa_u \end{cases} \quad (11)$$

where:

σ_k – the yield stress at the kink point,

κ_k – the state variable at the kink point,

κ_u – the state variable at zero stress.

Alternatively, an exponential definition is used (Fig. 2b):

$$\sigma_y(\kappa) = f_t \exp\left(-\frac{\kappa}{\kappa_u}\right) \quad (12)$$

where:

κ_u – controls the slope of the curve.

More advanced exponential relationship was proposed by Hordijk ([14]) based on experimental outcomes.

In eXtended Finite Element Method, state variables κ_k (only for bilinear softening) and κ_u can be directly related to the initial fracture energy G_f and the total fracture energy G_F . The initial fracture energy G_f (Bažant [1]) is the area under the initial tangent line from the peak at the stress – displacement curve (grey regions in Fig. 2), while the total fracture energy G_F is the area under the whole curve. In bilinear softening these parameters can be derived as:

$$\kappa_k = \frac{2G_f}{f_t^2} (f_t - \sigma_k) \quad (13)$$

and:

$$\kappa_u = \frac{2}{\sigma_k} \left(G_F + G_f \left(\frac{\sigma_k}{f_t} - 1 \right) \right) \quad (14)$$

while in exponential softening:

$$\kappa_u = \frac{G_F}{f_t} \quad (15)$$

PROBLEM

In the paper the experiment performed by Hoover et al. [15] is numerically simulated. They examined 128 unnotched and notched plain concrete beams under three-point bending. Figure 3 presents the geometry of a beam. Four different beam sizes were tested with height (depth) D taken as 500,

215, 93 and 40 mm, labelled here as a huge, large, medium and small specimen, respectively. The length to depth ratio was kept constant and it was equal to 2.4 for all beams and the span length L was defined as $2.176D$. Five different notch to depth ratios α_0 were assumed: 0.0 (no notch), 0.025, 0.075, 0.15 and 0.30. In total 18 different geometries were defined (small and medium beams with the ratio $\alpha_0=0.025$ were not cast). The thickness of all beams was $B=40$ mm and the width of the notch was equal to 1.5 mm for all specimens.

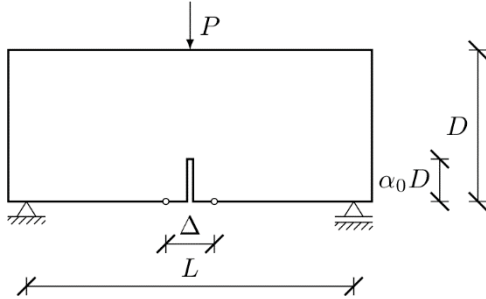


Fig. 3. Boundary conditions and geometry of a beam

A load was imposed in the middle of the top edge of the specimen. Steel plates were placed at supports and under the load. A hard (rigid) contact was assumed between concrete and steel plates at the supports and under the load. All tests were executed under crack mouth opening displacement control by increasing the distance between two chosen points at the bottom edge symmetrically with the respect to vertical axis of symmetry. The initial distance between these two points depended on the beam size D and the ratio α_0 (it was between 12.7 and 162 mm).

FE-CALCULATIONS

INPUT DATA

Numerical simulations are performed in Abaqus Standard programme. The total elongation of the gauge is set to $\Delta=0.3$ mm and an indirect displacement method is used. At least 250 increments are required to complete a simulation. Plane stress conditions are assumed with 3-node constant strain triangular finite elements. In elasto-plasticity an approximated method is used in calculations of averaged quantities. In an integration point the influence of the neighbour points is determined with values from the previous iteration. The refined FE mesh along the vertical axis of symmetry is defined in all specimens with the maximum element size not greater than 1 mm for calculations with elasto-plasticity and 2 mm for XFEM simulations. The total number of finite elements varies between 6967 and 55251 and between 4981 and 11660 in calculations with smeared and discrete cracks, respectively. A denser FE-mesh for calculations with elasto-plasticity ensures the effective

application of the non-local theory ever for small values of the characteristic lengths and obtaining mesh independent results. Some comparative simulations with XFEM have shown that identical results have been received using coarser and denser meshes. An exemplary FE-mesh used in XFEM calculations in the region around the notch for the medium beam and the notch to depth ratio $\alpha_0=0.15$ is shown in Fig. 4.

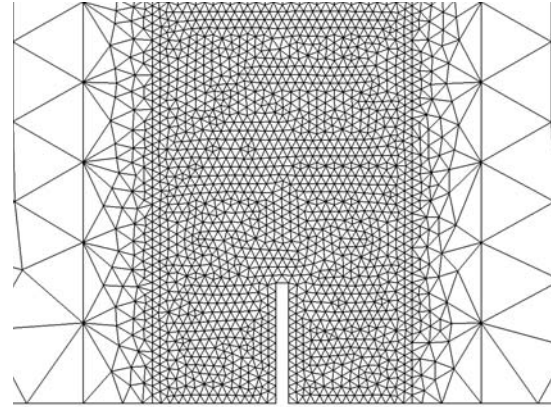


Fig. 4. Exemplary FE mesh around the notch

In the simulations the Young's modulus is assumed as $E=41.25$ GPa and the Poisson's ratio is $\nu=0.172$ (taken from experiments by Hoover et al. [15]). The total fracture energy is set to $G_f=70$ N/m (after Hoover and Bažant [16]). In bilinear softening the yield stress at the kink point is always defined as $\sigma_k=0.15f_t$. In XFEM the drop factor is equal to $d_f=10^4$ and the shear stiffness is $T_s=0.0$ N/m³. Material for steel plates is taken as a linear elastic with the Young's modulus $E_s=200$ GPa and the Poisson's ratio $\nu_s=0.3$.

RESULT AND ERROR MEASURES

The experimental nominal (ligament) strength σ_N^{exp} is calculated as:

$$\sigma_N^{\text{exp}} = \frac{3}{2} \frac{2.176 P_u^{\text{exp}}}{B^{\text{exp}} D^{\text{exp}}} \quad (16)$$

where:

P_u^{exp} – the experimental max. force,

B^{exp} – the experimental thickness,

D^{exp} – the experimental height.

The numerical nominal strength σ_N^{FEM} is defined as:

$$\sigma_N^{\text{FEM}} = C_f \frac{3}{2} \frac{2.176 P_u^{\text{FEM}}}{BD} \quad (17)$$

where:

P_u^{FEM} – the numerical max. force,

C_f – the correction factor.

The correction factor takes into account deviations of real dimensions with the respect to nominal ones. It is defined as:

$$C_f = \frac{2}{3} \frac{\sigma_N^{\text{exp}} BD}{2.176 P_u^{\text{exp}}} \quad (18)$$

In order to rate a simulation quality, the following relative error Err_0 is introduced:

$$Err_0 = \frac{\sigma_N^{\text{FEM}} - \sigma_N^{\text{exp}}}{\sigma_N^{\text{exp}}} \quad (19)$$

The whole set is evaluated using errors Err_1 and Err_2 :

$$Err_1 = \sum_{i=1}^N \frac{Err_0}{N} \quad \text{and} \quad Err_2 = \sum_{i=1}^N \frac{|Err_0|}{N} \quad (20)$$

where:

N – the number of beams ($N=18$).

In statistics, the errors Err_1 and Err_2 are called the mean percentage error (MPE) and the mean absolute percentage error (MAPE), respectively. The presence of the negative error values allows for distinguish between underestimated and overestimated numerical results.

RESULTS WITH XFEM

First, simulations with bilinear softening curve are executed. In order to find the values of the tensile strength f_t and the initial fracture energy G_f , seed calculations are performed. The tensile strength f_t changes between 3.6 MPa and 5.6 MPa with an increment 0.4 MPa. The initial fracture energy G_f varies between 30 N/m and 54 N/m with an increment 2 N/m. Obtained error Err_1 and Err_2 isolines are depicted at Fig. 5. It can be seen that for both measures the best f_t and G_f pairs form an inclined line (or region), but they do not indicate a single optimum point. Please note, however, that not only peak values, but also agreement between whole numerical and experimental curves has to be taken into account. Finally, the tensile strength is set to $f_t=5.0$ MPa and the initial fracture energy is taken as $G_f=48$ N/m. With these values the following errors are obtained: $Err_1=0.67\%$ and $Err_2=2.69\%$. Figure 6a presents a comparison between nominal strength obtained in the experiment and FE-calculations. Generally, a very good agreement can be observed. The largest deviation (the error $Err_0=10.7\%$) is for the small beam ($D=40$ mm) and the notch to depth ratio $\alpha_0=0.3$. Whole force – displacement curves are presented in Fig. 7. It can be seen that numerical results fit nicely into experimental ranges (grey regions). This fact confirms the proper assumption of the total fracture energy $G_F=70$ N/m.

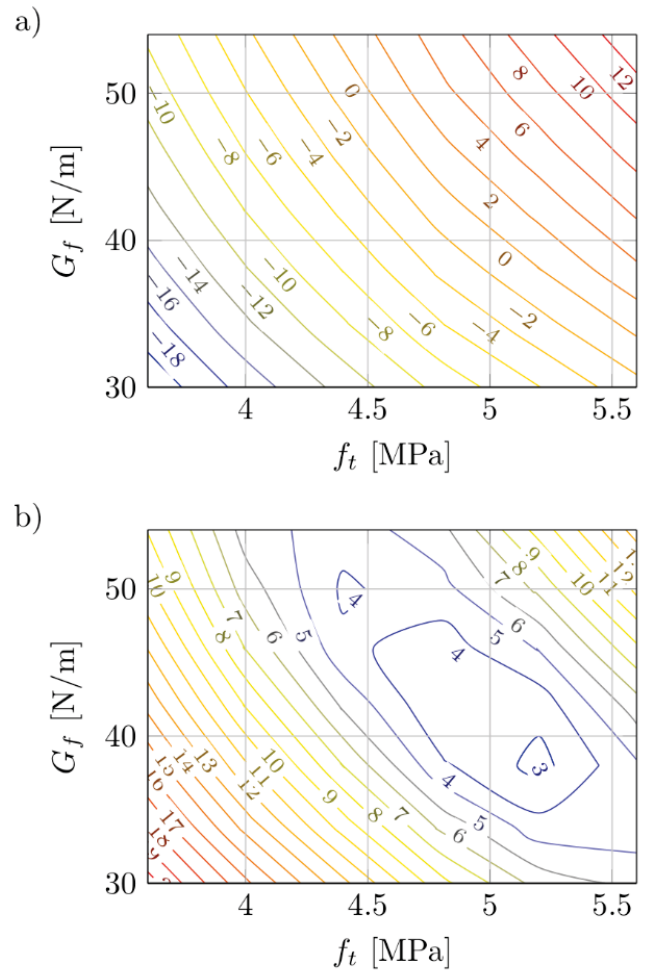


Fig. 5. Error contour maps for seed calculations with XFEM: Err_1 (a) and Err_2 (b) (in percentages)

The performance of the exponential softening curve with the following parameters: $f_t=4.8$ MPa and $G_f=35$ N/m is studied also (values based on some initial calculations). In the case of the exponential softening, there is no possibility to control independently both: initial G_f and total G_F fracture energies. The initial fracture energy G_f is always equal to 50% of the total fracture energy G_F . FE-calculations with above parameters produce the following errors: $Err_1=0.20\%$ and $Err_2=3.65\%$, comparable to values obtained with the bilinear softening. Here the worst specimen is the huge beam ($D=500$ mm) and the notch to depth ratio $\alpha_0=0.3$; it gives the error $Err_0=8.9\%$. Comparison between experimental and numerical nominal strength is done in Fig. 6b. Again, a good agreement is achieved (here some differences occur also for unnotched beams).

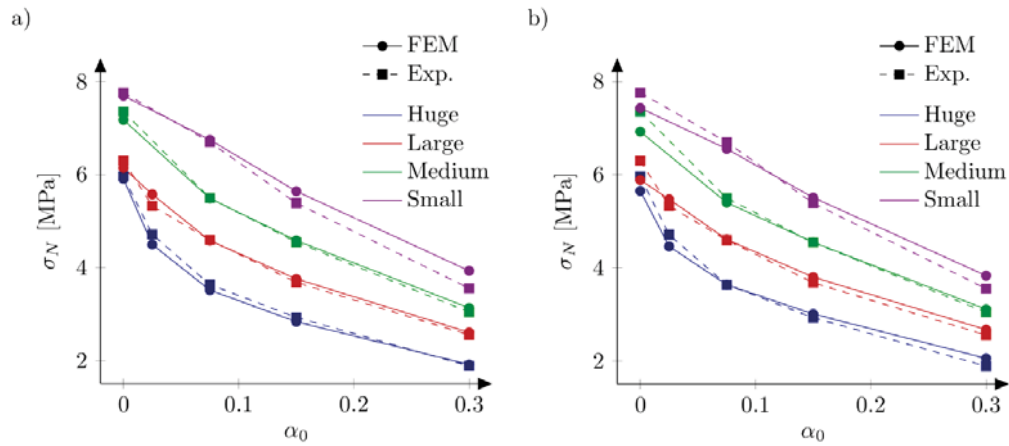


Fig. 6. Nominal (XFEM calculations) and experimental strengths with the bilinear softening curve, $f_t=5.0$ MPa and $G_f=48$ N/m (a) and the exponential softening, $f_t=4.8$ MPa and $G_f=35$ N/m (b)

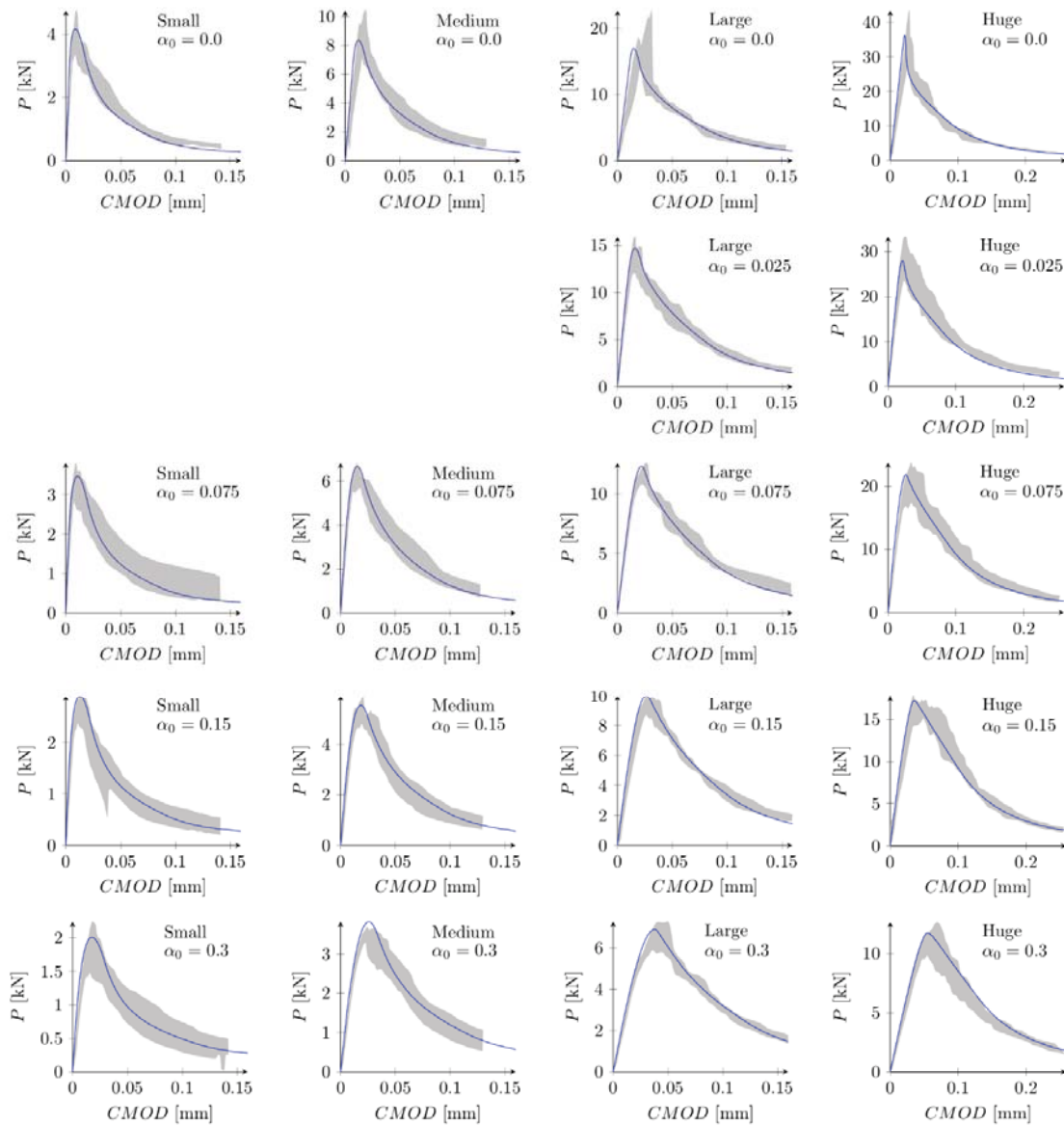


Fig. 7. Experimental and numerical (XFEM calculations) force - crack mouth opening displacement (CMOD) curves for bilinear softening, $f_t=5.0$ MPa and $G_f=48$ N/m

RESULTS WITH ELASTO-PLASTICITY

Next the numerical simulations are repeated with the elasto-plastic constitutive law with a Rankine criterion. Two characteristic lengths are assumed: $l=5$ mm and $l=2$ mm. The values of κ_u (for both softening curve definitions) are chosen in such a way to obtain the identical force-displacement curves with XFEM and elasto-plastic model with any of two characteristic lengths analysed. In calculations with the bilinear softening the ultimate value of the state variable is taken as $\kappa_u=4.05 \cdot 10^{-3}$ and $\kappa_u=10.13 \cdot 10^{-3}$ for the characteristic length $l=5$ mm and $l=2$ mm, respectively (to obtain initial fracture energy $G_f=48$ N/m). The tensile strength is $f_t=5.0$ MPa (as in XFEM calculations). Simulations give the following errors: $Err_1=Err_2=9.76\%$ for the characteristic length $l=5$ mm and $Err_1=Err_2=6.80\%$ for the characteristic length $l=2$ mm. Comparison between numerical and experimental nominal strengths is made in Fig. 8. In general, both parameter sets overestimate experimental outcomes. The worst specimen returns errors $Err_0=28.1\%$ and $Err_0=19.2\%$ (the small beam with $\alpha_0=0.3$). Fortunately, the overestimation reduces with decreasing the characteristic length. It suggests the smaller values should be assumed in simulations.

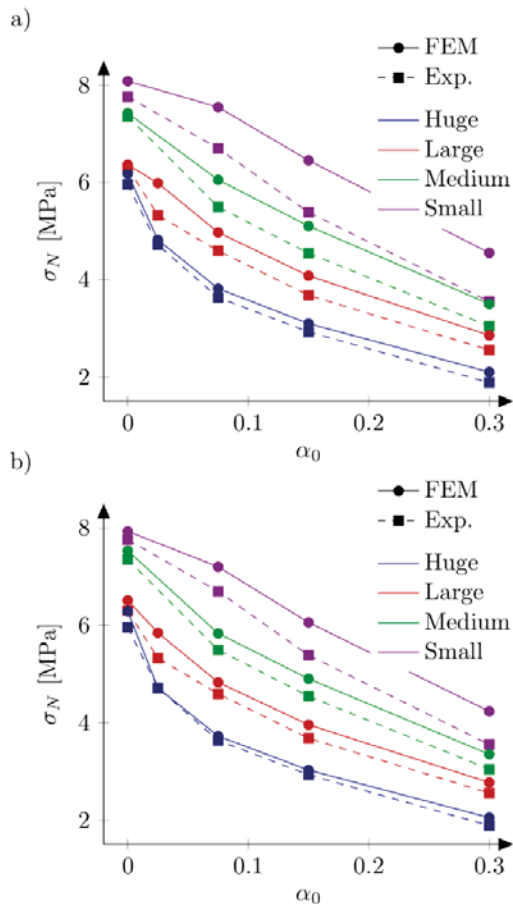


Fig. 8. Nominal (elasto-plasticity calculations) and experimental strengths with the bilinear softening curve, $f_t=5.0$ MPa, $G_f=48$ N/m and the characteristic length $l=5$ mm (a) and $l=2$ mm (b)

Slightly better results are obtained from simulations with the exponential softening law. Here the ultimate value of the softening parameter is assumed as $\kappa_u=0.758 \cdot 10^{-3}$ and $\kappa_u=1.894 \cdot 10^{-3}$ for the characteristic length $l=5$ mm and $l=2$ mm, respectively (to obtain initial fracture energy $G_f=35$ N/m). The tensile strength is $f_t=4.8$ MPa (as in XFEM calculations). The following errors are returned: $Err_1=4.91\%$ and $Err_2=6.82\%$ for the characteristic length $l=5$ mm and $Err_1=2.43\%$ and $Err_2=4.16\%$ for the characteristic length $l=2$ mm. Again, in general too high peak loads are obtained in calculations, although last errors Err_2 is already comparable with error values produced in XFEM simulations. Figure 9 presents a comparison between numerical and experimental nominal strengths, while force - CMOD curves are shown in Fig. 10. Despite the overestimation of peak loads, numerical curves fit into experimental limits.

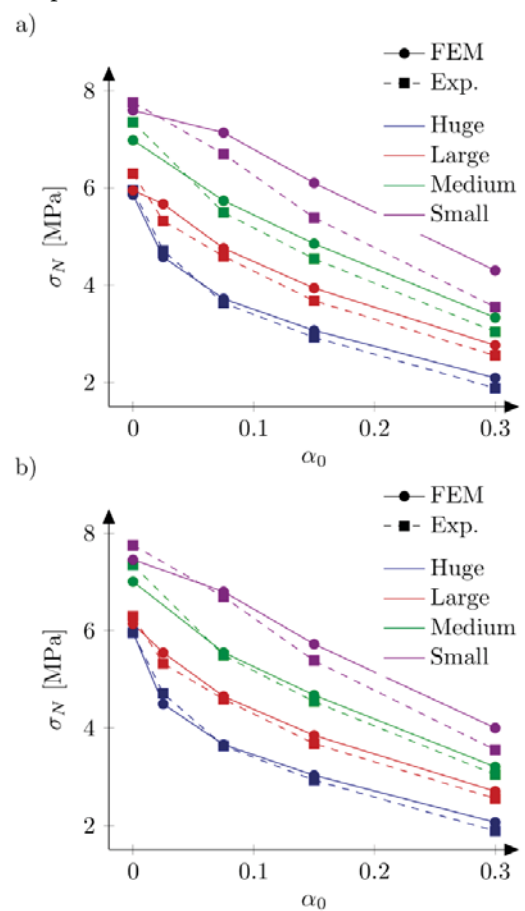


Fig. 9. Nominal (elasto-plasticity calculations) and experimental strengths with the exponential softening curve, $f_t=4.8$ MPa, $G_f=35$ N/m and the characteristic length $l=5$ mm (a) and $l=2$ mm (b)

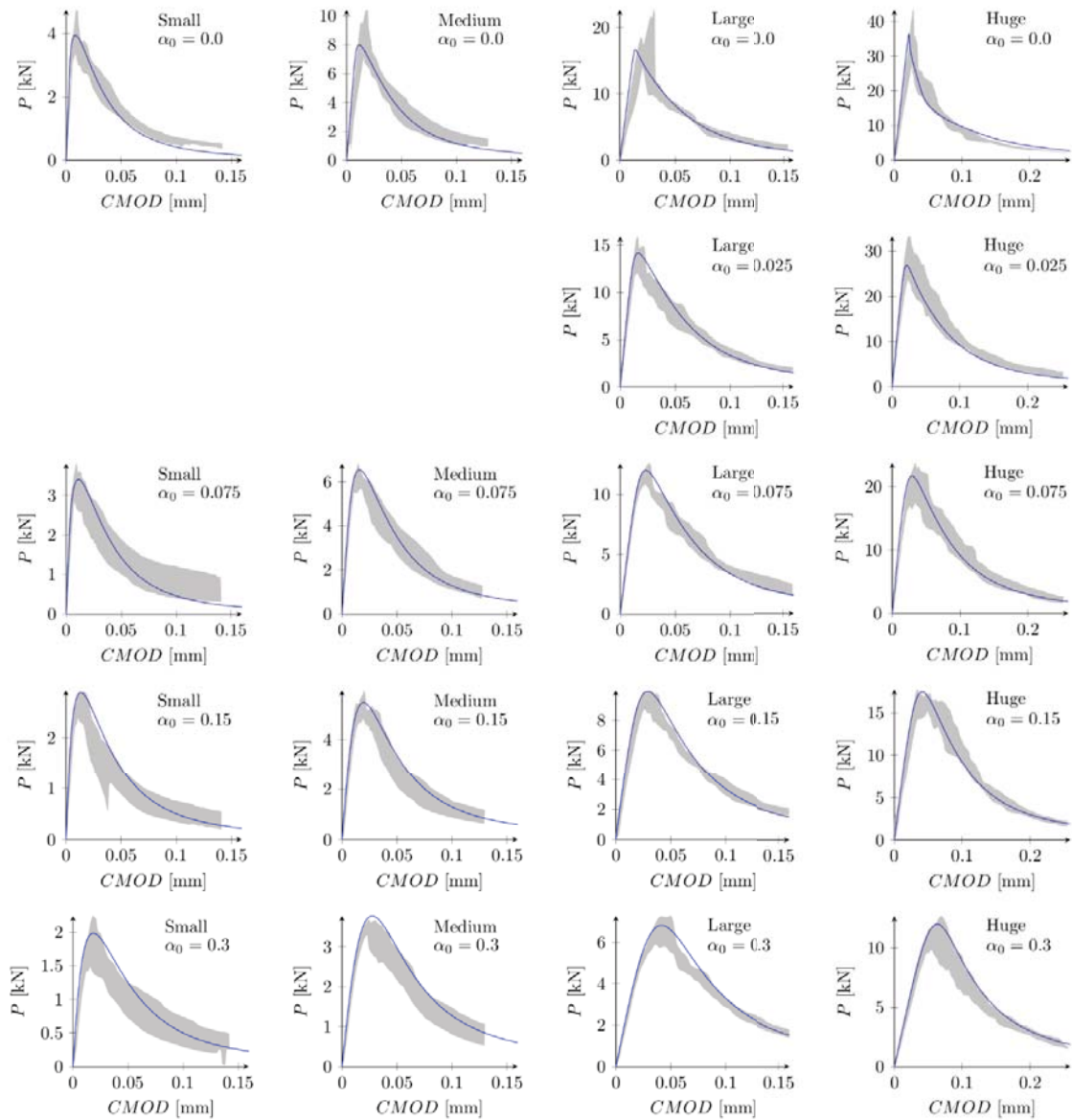


Fig. 10. Experimental and numerical (elasto-plasticity calculations) force – crack mouth opening displacement (CMOD) curves for exponential softening, $f_t=4.8$ MPa and $G_f=35$ N/m

CONCLUSIONS

In the paper the size effect phenomenon in plane concrete beams under bending has been investigated. The numerical calculations using smeared and discrete methods describing cracks in concrete have been executed. Obtained results have been compared with experimental outcomes. Both approaches gave results consistent with experiments, although smaller errors have been attained with XFEM. In elasto-plasticity, simulations with smaller values of the characteristic length have returned better results (smaller errors have been obtained). Both softening curves have produced comparable

results, assuming different initial fracture energies. This observation points some problems in unique identification of the initial fracture energy, when different curve definitions in softening are used. When assuming a curved softening relationship (e.g. exponential one) purely geometrical definition of the initial fracture energy is not sufficient and the curvature of the curve in the domain after the peak should be taken into account.

The ongoing research is focused on improving the agreement of numerical results obtained with elasto-plastic constitutive law with experimental curves. More advanced, anisotropic averaging schemes in non-locality proposed by Giry et al. [9] and Grassl et al. [11] are investigated. The consequences of decreasing the fracture energy in the boundary layer (Bažant et al. [2]) are also examined.

ACKNOWLEDGEMENTS

Calculations were carried out at the Academic Computer Centre in Gdańsk.

BIBLIOGRAPHY

1. Bažant Z.P.: *Concrete fracture modelling: testing and practice*. Engineering Fracture Mechanics 2002; 69:165-206.
2. Bažant Z.P., Le J.-L., Hoover C.G.: *Nonlocal boundary layer (NBL) model: overcoming boundary condition problems in strength statistics and fracture analysis of quasibrittle materials*. Proceedings of the 7th International Conference on Fracture Mechanics of Concrete and Concrete Structures 2010; 135-143.
3. Beda P.B.: *Dynamical Systems Approach of Internal Length in Fractional Calculus*. Engineering Transactions 2017, 65:209-215.
4. Błaszczyk T.: *Analytical and numerical solution of the fractional Euler-Bernoulli beam equation*. Journal of Mechanics of Materials and Structures 2017; 12:23-34.
5. Bobiński J., Tejchman J.: *A coupled constitutive model for fracture in plain concrete based on continuum theory with non-local softening and eXtended Finite Element Method*. Finite Elements in Analysis and Design 2016; 114:1-21.
6. Brinkgreve R.B.J.: *Geomaterial models and numerical analysis of softening*. PhD Thesis, TU Delft 1994.
7. Çağlar Y., Şener S.: *Size effect tests of different notch depth specimens with support rotation measurements*. Engineering Fracture Mechanics 2016; 157:43-55.
8. Cox J.V.: *An extended finite element method with analytical enrichment for cohesive crack modelling*. International Journal for Numerical Methods in Engineering 2009; 78:48-83.
9. Giry C., Dufour F., Mazars J.: *Stress-based nonlocal damage model*. International Journal of Solids and Structures 2011; 48:3431-3443.
10. Glema A., Łodygowski T., Perzyna P.: *Interaction of deformation waves and localization phenomena in inelastic solids*. Computer Methods in Applied Mechanics and Engineering 2000; 183:123-140.
11. Grassl P., Xenos D., Jirásek M., Horák M.: *Evaluation of nonlocal approaches for modelling fracture near nonconvex boundaries*. International Journal of Solids and Structures 2014; 51:3239-3251.
12. Grégoire D., Rojas-Solano L., Pijaudier-Cabot G.: *Failure and size effect for notched and unnotched concrete beams*. International Journal for Numerical and Analytical Methods in Geomechanics 2013; 37:1434-1452.
13. Havlásek P., Grassl P., Jirásek M.: *Analysis of size effect on strength of quasi-brittle materials using integral-type nonlocal models*. Engineering Fracture Mechanics 2016; 157:72-85.
14. Hordijk D.A.: *Local approach to fatigue of concrete*. PhD Thesis, TU Delft 1991.
15. Hoover C.G., Bažant Z.P., Vorel J., Wendner R., Hubler M.H.: *Comprehensive concrete fracture tests: Description and results*. Engineering Fracture Mechanics 2013; 114:92-103.
16. Hoover C.G., Bažant Z.P.: *Cohesive crack, size effect, crack band and work-of-fracture models compared to comprehensive concrete fracture tests*. International Journal of Fracture 2014; 187:133-143.
17. Lazopoulos K.A., Lazopoulos A.K.: *Fractional vector calculus and fluid mechanics*. Journal of the Mechanical Behavior of Materials 2017; 26:43-54.
18. Marzec I., Skarżyński Ł., Bobiński J., Tejchman J.: *Modelling reinforced concrete beams under mixed shear-tension failure with different continuous FE approaches*. Computers and Concrete 2013; 12:585-612.
19. Marzec I., Tejchman J., Winnicki A.: *Computational simulations of concrete behaviour under dynamic conditions using elasto-visco-plastic model with non-local softening*. Computers and Concrete 2015; 15(4):515-545.
20. Mazars J., Hamon F., Grange S.: *A new 3d damage model for concrete under monotonic, cyclic and dynamic load*. Materials and Structures 2015; 48:3779-3793.
21. Melenk J.M., Babuška I.: *The partition of unity finite element method: basic theory and applications*. Computer Methods in Applied Mechanics and Engineering 1996; 139:289-314.
22. Simone A., Wells G.N., Sluys L.J.: *From continuous to discontinuous failure in a gradient-enhanced continuum damage model*. Computer Methods in Applied Mechanics and Engineering 2003; 192:4581-4607.
23. Simone A., Sluys L.J.: *The use of displacement discontinuities in a rate-dependent medium*. Computer Methods in Applied Mechanics and Engineering 2004; 193:3015-3033.
24. Sumelka W.: *Non-local Kirchhoff-Love plates in terms of fractional calculus*. Archives of Civil and Mechanical Engineering 2015; 15:231-242.

25. Sumelka W., Błaszczak T., Liebold C.: Fractional Euler–Bernoulli beams: Theory, numerical study and experimental validation. *European Journal of Mechanics - A/Solids* 2015; 54:243-251.
26. Unger J.F., Eckardt S., Könke C.: *Modelling of cohesive crack growth in concrete structures with the extended finite element method*. *Computer Methods in Applied Mechanics and Engineering* 2007; 196:4087–4100.
27. Wang W.M., Sluys L.J., de Borst R.: *Viscoplasticity for instabilities due to strain softening and strain-rate softening*. *International Journal for Numerical Methods in Engineering* 1997; 40:3839-3864.
28. Wells G.N., Sluys L.J.: *A new method for modelling cohesive cracks using finite elements*. *International Journal for Numerical Methods in Engineering* 2001; 50:2667-2682.
29. Winnicki A., Pearce C.J., Bićanić N.: *Viscoplastic Hoffman consistency model for concrete*. *Computers & Structures* 2001; 79:7-19.
30. Zi G., Belytschko T.: *New crack-tip elements for XFEM and applications to cohesive cracks*. *International Journal for Numerical Methods in Engineering* 2003; 57:2221-2240.

CONTACT WITH THE AUTHORS

Ireneusz Marzec

e-mail: irek@pg.edu.pl

Gdansk University of Technology
Narutowicza 11/12, 80-233 Gdańsk

POLAND

Jerzy Bobiński

e-mail: bobin@pg.edu.pl

Gdansk University of Technology
Narutowicza 11/12, 80-233 Gdańsk

POLAND